

AD-780 033

PLASMA MODIFICATION ASSOCIATED
WITH PARAMETRIC INSTABILITIES DRIVEN
BY INTENSE ELECTROMAGNETIC WAVES

James T. Flick, et al

Princeton University

Prepared for:

Home Air Development Center
Advanced Research Projects Agency

April 1974

DISTRIBUTED BY:

NTIS

National Technical Information Service
U. S. DEPARTMENT OF COMMERCE
5285 Port Royal Road, Springfield Va. 22151

Unclassified

SECURITY CLASSIFICATION OF THIS PAGE (When Data Entered)

REPORT DOCUMENTATION PAGE		READ INSTRUCTIONS BEFORE COMPLETING FORM	
1 REPORT NUMBER RADC-TR-74-126	2 GOVT ACCESSION NO.	3 RECIPIENT'S CATALOG NUMBER AD-780 033	
4 TITLE (and Subtitle) Plasma Modification Associated with Parametric Instabilities Driven by Intense Electromagnetic Waves		5 TYPE OF REPORT & PERIOD COVERED Final Report	
		6 PERFORMING ORG. REPORT NUMBER	
7 AUTHOR(s) James T. Flick Hans W. Hendel		8 CONTRACT OR GRANT NUMBER(s) F30602-73-C-0163	
9 PERFORMING ORGANIZATION NAME AND ADDRESS Princeton University, Plasma Physics Laboratory James Forrestal Campus P. O. Box 451, Princeton, New Jersey		10 PROGRAM ELEMENT PROJECT, TASK AREA & WORK UNIT NUMBERS 14231003	
11 CONTROLLING OFFICE NAME AND ADDRESS Defense Advanced Research Projects Agency 1400 Wilson Blvd. Arlington, Virginia 22209		12 REPORT DATE April 1974	
		13 NUMBER OF PAGES	
14 MONITORING AGENCY NAME & ADDRESS (if different from Controlling Office) Rome Air Development Center (OCSE) Griffiss Air Force Base New York 13441		15 SECURITY CLASS. (of this report) Unclassified	
		15a DECLASSIFICATION/DOWNGRADING SCHEDULE	
16 DISTRIBUTION STATEMENT (of this Report) Approved for Public Release; Distribution Unlimited			
17 DISTRIBUTION STATEMENT (of the abstract entered in Block 20, if different from Report)			
18 SUPPLEMENTARY NOTES			
19 KEY WORDS (Continue on reverse side if necessary and identify by block number) Anomalous Absorption Parametric Ion Acoustic Decay Instability			
20 ABSTRACT (Continue on reverse side if necessary and identify by block number) The isothermal ($T_e = T_i$) parametric ion acoustic decay instability, expected to cause modification of the ionosphere upon irradiation by intense electromagnetic waves $\omega_0 \approx \omega_{pe}$, has been studied in detail in laboratory Q-machine plasmas. The instability is conclusively identified by wavelength and frequency measurements, over all parameter ranges ($k_{de} \leq 0.2$; $\omega_{Lp}/\omega_{pi} \approx 1$). Other parameters determined are instability threshold and maximum acoustic frequency dependence upon density; instability bandwidths and spatial profiles; electron and ion heating--all in agreement with linear, homogeneous theory. Not in agreement with theory are			

DD FORM 1 JAN 73 1473

EDITION OF 1 NOV 65 IS OBSOLETE

Unclassified

SECURITY CLASSIFICATION OF THIS PAGE (When Data Entered)

Unclassified

SECURITY CLASSIFICATION OF THIS PAGE(When Data Entered)

relations between L_r , HF and pump intensities.

Significant enhancement of the plasma RF resistivity occurs when the HF instability field amplitude becomes comparable to or larger than the pump field amplitude. When this occurs, energy absorbed by the plasma directly from the pump and indirectly from the instability are of the same order. Since pump energy must be expended to maintain the instability, the result is an effective enhancement of the plasma resistivity. Energy loss from the strong ion Landau damping of ion acoustic LF waves can be neglected, due to the small acoustic intensity. In these experiments, resistivity enhancement greatly exceeds reduction due to electron temperature increase from plasma heating.

Also associated with instability onset are observations of strong ion and electron heating. Significant ion temperature increase, in times short compared to collisional heating times, is shown to be due to stochastic heating by the random fields of the instability LF spectrum. Most of the pump energy goes into (conventional RF) heating of electrons; however, due to the very high electron thermal conductivity, and an essentially infinite electron heat sink at each end of the Q-machine plasma, isothermal temperature characteristics are maintained, even for pump powers well above threshold.

Unclassified

SECURITY CLASSIFICATION OF THIS PAGE(When Data Entered)

//

SAC--Griffins AFB NY

PLASMA MODIFICATION ASSOCIATED WITH PARAMETRIC
INSTABILITIES DRIVEN BY INTENSE ELECTROMAGNETIC WAVES

James T. Flick
Hans W. Hendel

Contractor: Princeton University
Contract Number: F30602-73-C-0163
Effective Date of Contract: 20 February 1973
Contract Expiration Date: 31 December 1973
Amount of Contract: \$45,000.00
Program Code Number: 3E20

Principal Investigator: Melvin B. Gottlieb
Phone: 609 452-5600

Project Engineer: Vincent J. Coyne
Phone: 315 330-3141

Contract Engineer: Frederick C. Wilson
Phone: 315 330-3085

Approved for public release;
distribution unlimited.

This research was supported by the
Defense Advanced Research Projects
Agency of the Department of Defense
and was monitored by Frederick C.
Wilson RADC (OCSE), GAFB, NY 13441
under Contract F30602-73-C-0163.

PUBLICATION REVIEW

This technical report has been reviewed and is approved.

Fredrick C. Wilson
RADC Project Engineer

Plasma Modification Associated with Parametric
Instabilities Driven by Intense Electromagnetic Waves

James T. Flick and Hans W. Hendel
Plasma Physics Laboratory, Princeton University
Princeton, New Jersey 08540

ABSTRACT

The isothermal ($T_e \approx T_i$) parametric ion acoustic decay instability, expected to cause modification of the ionosphere upon irradiation by intense electromagnetic waves $\omega_0 \lesssim \omega_{pe}$, has been studied in detail in laboratory Q-machine plasmas. The instability is conclusively identified by wavelength and frequency measurements, over all parameter ranges ($k\lambda_{de} \leq 0.2$; $\omega_{LF}/\omega_{pi} \leq 1$). Other parameters determined are instability threshold and maximum acoustic frequency dependence upon density; instability bandwidths and spatial profiles; electron and ion heating--all in agreement with linear, homogeneous theory. Not in agreement with theory are relations between LF, HF and pump intensities.

Significant enhancement of the plasma RF resistivity occurs when the HF instability field amplitude becomes comparable to or larger than the pump field amplitude. When this occurs, energy absorbed by the plasma directly from the pump and indirectly from the

I. SUMMARY

The purpose of the experimental effort at Princeton University is to study, in laboratory plasma, effects relating to observations of enhanced absorption of electromagnetic waves in the ionosphere. (A review paper on "Laboratory Parametric Instability Experiments" has been published in Comments on Plasma Physics, see Ref. 1.) The experiments were performed in a Q-machine plasma, which has comparable ion and electron temperatures, similar to the ionosphere.

Excitation of the parametric ion acoustic decay instability occurs when an exciting RF electric field E_0 ($\omega_0 \lesssim \omega_{pe}$) exceeds a threshold value in agreement with predictions from linear theory. The instability spectrum consists of simultaneously excited high frequency ($\omega_{HF} = \omega_0 - \omega_{LF}$) and low frequency ($\omega_{LF} = \omega_{acoustic} \lesssim \omega_{pi} \ll \omega_{HF}$) bands. The enhanced collision frequency (anomalous RF resistivity) was measured by cavity Q determinations, and by extension of the cavity work to direct probe measurements of instability and pump amplitudes. Cavity Q measurements showed onset of anomalous resistivity, for $v_{de}/v_{the} \approx 0.05$ in good agreement with instability threshold predictions from infinite homogeneous theory. (See Ref. 2, Phys. Rev. Lett. 29, 634 (1972)). More recent measurements show strong resistivity enhancement evolving after several instability growth periods, the enhancement increasing strongly with pump electric field. At higher pump intensities, (10 x threshold) significantly

greater than those reported in the previous cavity work, instability saturation, $\langle E_{\text{instHF}}^2 \rangle \approx E_0^2$, leads to saturation of the anomalous resistivity.

Significant ion and electron heating (Phys. Rev. Lett. 31, 199 (1973), see Ref. 3) is observed, with intensities about ten times threshold, maintaining $T_e/T_i \approx 1$, and severe ion Landau damping of acoustic waves. The intense heating also leads to reduction of the plasma density, due to changes in the axial transport properties.

greater than those reported in the previous cavity work, instability saturation, $\langle E_{\text{instHF}}^2 \rangle \approx E_0^2$, leads to saturation of the anomalous resistivity.

Significant ion and electron heating (Phys. Rev. Lett. 31, 199 (1973), see Ref. 3) is observed, with intensities about ten times threshold, maintaining $T_e/T_i \approx 1$, and severe ion Landau damping of acoustic waves. The intense heating also leads to reduction of the plasma density, due to changes in the axial transport properties.

II. INTRODUCTION

One of the primary physical mechanisms proposed for the observed ionospheric modification by intense electromagnetic waves has been excitation of parametric instabilities.⁴ However, direct, conclusive identification of the specific heating mechanism in the ionosphere is difficult due to its inaccessibility. For this reason, laboratory programs have been set up to duplicate, as completely as possible, conditions in the ionosphere. Since one of the dominant characteristics of the ionospheric plasma is the comparable ion and electron temperature, which should cause severe ion Landau damping of acoustic waves, identification of the acoustic waves, and thus of the ion acoustic decay instability under these conditions is essential. In addition, the instability characteristics might be different from an instability where all waves involved are weakly damped. For this reason, the Princeton experimental program has been directed to the conclusive identification of the ion acoustic decay instability in an isothermal plasma, and of its properties, in an attempt to model the dominant characteristics of the ionospheric heating experiments.

Although work in this area is complicated by the severe ion Landau damping of acoustic waves, our results identify the ion acoustic decay instability, and demonstrate its strong effects on plasma heating and modification, as predicted. Due to the severe ion damping, this instability has properties quite different from the ion acoustic instability in a plasma with cool ions.

III. EXPERIMENT

Machine Parameters

The plasma device used is the Princeton "Q-1" machine (Fig. 1). Summarizing the equilibrium conditions: The alkali metal (K,Cs) 1 m long x 3 cm diameter plasma is produced at each end by contact ionization of neutral atoms, and thermionic emission of electrons from hot tungsten end plates ($T_i \approx T_e \approx T_{pl} = 0.2$ eV) oriented perpendicular to the axial confining magnetic field ($\omega_{pe}/\omega_{ce} \leq 3$). Plasma production from each end is balanced, so that no equilibrium ion or electron drifts are present. Neutral collisions are negligible, since the neutral pressure is cryogenically reduced below 10^{-7} Torr.

Frequency and amplitude measurements are made with special HF probes. Electron temperature measurements are performed with Langmuir probes--when the RF perturbation effect on this measurement is serious, a standing wave line is used to tune out the RF potential. Ion temperatures are determined with probes that mechanically suppress the electron saturation current.⁵ Wavelength measurements are made either with an axial probe ($k_{||} < 15$ cm⁻¹) or with rotary double probes ($k < 70$ cm⁻¹) and sensitive, specially constructed HF and LF interferometer systems.

Parametric Instability

The ion acoustic parametric decay instability, described in detail elsewhere⁶, is summarized briefly below:

The presence of a large-amplitude electromagnetic, or electrostatic (pump) wave in a plasma causes nonlinear (parametric) coupling between plasma normal modes--in this case, ion acoustic and electron plasma waves. When the pump intensity E_0^2 is raised above a critical level, E_{OC}^2 , HF and LF bands of the instability are parametrically excited, receiving energy from the pump field, and obeying the well-known frequency (energy) and wavenumber (momentum) conservation relations:

$$\begin{aligned}\omega_0 &= \omega_{LF} + \omega_{HF} \\ \vec{k}_0 &= \vec{k}_{LF} + \vec{k}_{HF}\end{aligned}\tag{1}$$

The effects of experimental conditions on the pump, HF, and LF modes are discussed briefly:

Pump ($\omega = \omega_0 \approx \omega_{pe}$)

The RF pump field (∞ wavelength \Rightarrow electromagnetic pump) is applied axially with a cavity or capacitive ring structure (Fig. 2). Due to the large ratio of the collisionless skin depth, $c/\omega [1 - (\omega_{pe}^2/\omega^2)]$, to plasma radius, a , perturbation effects by the plasma on the RF field can be neglected. However, the presence of plasma within a spatially localized axial RF field leads to linear mode conversion of the driving field into electrostatic waves. Significant coupling to axially propagating

electrostatic waves requires $k_{|| \text{E.S.}} \approx (1/E_{0||}) (\partial/\partial Z) E_{0||}$,⁷ (Fig. 3). Figure 4 shows the measured dispersion relation of these waves compared to theory for an $m = n = 0$, Gould-Trivelpiece wave corrected for the experimental radial plasma profile. Thus electrostatic, as well as electromagnetic excitation of the parametric instability must be considered.

HF Waves

Unstable HF waves ($\omega_{\text{HF}} \approx \omega_0$) are weakly damped electron plasma waves (lower hybrid branch, $0.1 < \omega/\omega_{\text{pe}} < 1$) in a strong magnetic field, satisfying the Gould-Trivelpiece dispersion relation, i.e., radial (n) and azimuthal (m) standing waves, allowing only discrete values of k_{HF} (Fig. 5). In the limit $m, n \rightarrow \infty$, the dispersion relation can be written:

$$\omega^2 = \omega_R^2 \left(\frac{k_{||}}{k} \right)^2 \quad (2)$$

$$\omega_R^2 = \omega_{\text{pe}}^2 + 3k^2 \frac{T_e}{m}$$

A number of significant points can be derived from this: First, these waves are reflected as they propagate radially out from the center of the plasma column. When azimuthal effects are neglected, reflection occurs at r_c , $\omega_{\text{pe}}^2(r_c) = \omega^2$; inclusion of azimuthal wavelengths reduces r_c even more. Second, evaluation of axial and radial damping lengths (of undriven HF waves) shows:

$$\frac{\text{Im } k_{\parallel}}{k} \approx \frac{\nu_{ei}}{\omega_R} \left(\frac{k}{k_{\perp}} \right)^2 \quad k\lambda_{de} < \frac{k_{\perp}}{k_{\parallel}}$$

$$\frac{\text{Im } k_{\perp}}{k} \approx \frac{\nu_{ei}}{\omega_R} \left(\frac{k}{k_{\parallel} k_{\perp}} \right)^2 \quad k\lambda_{de} < 1 \quad (3)$$

where $\text{Im } k$ is the damped part of a wave with wavenumber k , and, if $k_{\parallel} \approx k_{\perp} \approx k$, $(\text{Im } k) \approx \nu_{ei}/\omega_R = 10^{-3}$. Hence, the waves are weakly spatially damped, showing that k_{\perp} can have only discrete values under most experimental conditions, even when $k_{\perp} a \gg 1$. The condition for axial standing waves, however, is well-satisfied only for densities below $\approx 10^9 \text{ cm}^{-3}$. Since the HF waves are radial and azimuthal standing waves (no convective losses), homogeneous instability theory should apply.

LF Modes

Parametrically excited LF modes are ion acoustic waves in an unmagnetized plasma, ($\omega_{ci} \ll \omega_{LF} < \omega_{pi}$, $\rho_{Li} < a$). Due to the comparable ion and electron temperatures, these waves are severely ion Landau damped; in the notation of Fried and Gould,³ the collisionless dispersion relation becomes in the long wavelength limit ($k\lambda_d < 1$):

$$Z'(\omega/kv_{thi}) = \frac{2T_i}{T_e} \quad (4)$$

where Z is the plasma dispersion function. For $T_e = T_i$, the least damped root³ is:

$$\omega_{LF} = 2.1 k(T/M)^{1/2}$$

$$\frac{\nu_i}{\omega_{LF}} = 0.4 \quad (5)$$

This result compares favorably with collisional fluid theory:

$$\omega_{LF} = k(T_e + 3T_i/M)^{1/2} \approx \sqrt{2}k(T/M)^{1/2} \quad (6)$$

The low frequency acoustic waves are thus severely Landau damped, as expected, and are virtually unaffected by magnetic fields, or radial density gradients.⁹

IV. EXPERIMENTAL RESULTS

Identification: Wavelength and Frequency Measurements

Identification of the ion acoustic parametric decay instability in a plasma with $T_e \approx T_i$ is achieved by wavelength and frequency measurements. The expected frequency conservation relations are shown, for various pump powers, in Fig. 6. Note that although the HF and LF spectra are broad $\Delta\omega \approx \omega_{LF}/2$, the HF (electron plasma wave) spectrum is a mirror image of the LF (ion acoustic) spectrum, as expected from theory.

Typical acoustic wavelength measurements are shown in Fig. 7, demonstrating spatial coherence over at least three complete wavelengths. These results were obtained with a double rotary probe with 2 mm spacing, and a narrow bandwidth interferometer, permitting measurements of wavelength of a fraction of a millimeter. The coherence is unexpected, since the acoustic waves are severely Landau damped. A simple physical explanation follows: Since the HF modes are radial and azimuthal standing

waves, $k_{\perp m, n}$ is fixed by boundary conditions. In addition, since $\omega_{HF} \approx \omega_0 \gg \omega_{LF}$, ω_{HF} is also fixed to a very good approximation (Fig. 5) for each value of m, n . Finally, since all HF modes have discrete wavelengths, $\tilde{k}_{LF} = \tilde{k}_C - \tilde{k}_{HF}$ must also be coherent to satisfy momentum conservation. We note that this effect has made acoustic wavelength measurements possible. In isothermal plasmas where k_{HF} is not fixed, acoustic wavelength measurements would be extremely difficult.

The parametrically excited acoustic dispersion relation determined from these measurements is shown in Fig. 8, giving $\omega_{LF} = k_{LF} c_s$ where $c_s = (2.3 \pm 0.6) \times 10^5$ cm/sec, in good agreement with expectations. Also indicated are the wavelength matching conditions: $|k_{HF}| \approx |k_{LF}|$, $k_o \approx 0$. Note that $\omega_{LF} \leq \omega_{pi}/2$, $k_{\perp} \lambda_{de} \leq .2$. The second condition is expected from theoretical considerations, since $k \lambda_{de} > 0.2$ causes strong electron Landau damping of HF electron plasma waves.

Spatial Profile

Another interesting consequence of the severe LF damping can be seen in the instability radial profiles (Fig. 9). First the HF wave decays spatially in the radial direction due to the cut-off at $r_c(\omega/\omega_{pe})$. As ω/ω_{pe} is increased, r_c decreases as expected. In addition, the LF acoustic decay wave follows precisely the decay of the HF wave, in agreement with expectations for a wave that damps in approximately one wavelength when not parametrically driven by the pump and HF wave.

Density Dependence

The effects of density variation upon instability threshold E_{co}^2 and maximum instability frequency downshift ω_{LF} are shown in Figs. 10 and 11. As expected, $E_{co}^2 \propto n^{3/2 \pm 1/4}$, (Fig. 10) giving good agreement with the homogeneous theory over a wide range of densities. Threshold dependence upon acoustic damping can be neglected, since $v_{iLD}/\omega_{LF} \approx \text{constant}$, independent of density. Agreement of theoretical and experimental thresholds for a single density has been reported previously.² Maximum instability frequency shift from the pump frequency is shown to be $\omega_{LF} \approx \omega_{pi}$ (Fig. 11), as expected for the single decay instability, ruling out multiple-decay type processes that lead to ω_{LF}' or $\omega_0 - \omega_{HF} > \omega_{pi}$.

Acoustic Instability Regimes-Dependence Upon ω/ω_{pe}

General instability regimes are outlined in Fig. 12. Modes identified as ion acoustic decay instabilities can be separated into two main areas; one where all HF wavelengths are strongly affected by transverse boundary conditions ($m, n \approx 0$), and one where $m, n \gg 0$, i.e., HF boundary effects can be neglected. When $\omega/\omega_{pe} \approx 1$, $k_{\parallel} > k_{\perp}$, boundary conditions are important, and small changes in HF decay mode numbers cause large changes in k_{\parallel} (see also Fig. 5). Since the acoustic dispersion relation $\omega_{LF} = kc_s$ indicates that a large change in k causes equally large changes in ω_{LF} , this effect leads to well-separated instability peaks, one for each HF mode excited. Another acoustic regime exists for

$\omega/\omega_{pe} \leq 0.4$, as shown in Fig. 12. Here for the same acoustic frequency, HF radial and azimuthal mode numbers become much larger, since $k_{||}/k_{\perp} \approx \omega/\omega_{pe} < 1$. Now the effect of HF boundary conditions can be neglected, allowing the instability to choose the most unstable wavelength, in contrast to the previous case where only discrete wavelengths are allowed. In addition, in this regime, $k_0 \ll k_{inst}$, so instability excitation is essentially electromagnetic. As shown in Fig. 13, the maximum threshold frequency downshift (or acoustic frequency) is $\omega_{LF} \approx \omega_{pi}/5$ over a wide range of densities, with comparable instability bandwidth. At higher pump powers, the range of unstable frequencies increases to approximately $\omega_{pi}/2$, in agreement with other results. One surprising point is that even though $\omega_{LF} < v_{ei}$, only frequencies downshifted from the pump are observed, whereas linear parametric instability theory predicts comparable down- and up-shifted peaks for the experimental conditions. The three-wave decay model is thus applicable to the experiment over a wider range of experimental parameters than the theory would suggest.

This regime ($k_0 \approx 0$ -the "electromagnetic instability") is of particular interest, since it most closely approximates conditions of the ion acoustic decay instability in a uniform, infinite isothermal plasma, like the ionosphere. One should note, however, that the pump field has a significant component transverse to the confining magnetic field. The instability also propagates transversely, so one might expect the effect of radial

density inhomogeneity to be important. Since the HF waves are transverse standing waves radial convective effects can be neglected. In addition, as Fig. 9 shows, the instability frequency is essentially independent of radial position, supporting the fact that all radial inhomogeneity effects can be neglected, ensuring applicability to ionospheric plasma.

Instability Growth and Saturation, Pump Depletion

An area of considerable interest is the time evolution of the ion acoustic decay instability, and its final saturated state. For example, if relations between LF, HF instability, and pump intensities are known, one can easily determine ion, and electron heating rates, pump depletion, and enhancement of RF heating efficiency, often described in the literature as anomalous RF resistivity. Some of the results of work in this area are described in Ref. 2. More recent work is presented in detail, covering instability growth, saturation, and power balance.

Growth Measurements

Discussing first instability growth, we note that due to the small amplitudes of acoustic waves, LF growth measurements are very difficult. At the high frequency, the large pump amplitude interferes, but can be tuned out with a homodyne technique, with a severe loss in sensitivity. Results are shown in Fig. 14(a) demonstrating growth and decay of the acoustic LF instability; just above threshold; as expected, instability growth

occurs with a rate $\gamma \approx \omega_{LF} \approx \omega_{pi}$, and decay $\nu_i \approx \omega_{LF}$, consistent with the picture of severely ion Landau damped acoustic waves. Note that initially the instability is coherent. After approximately 10-20 acoustic periods (Fig. 14(b)), the instability becomes incoherent, consistent with steady-state spectral observations.

Steady-State Measurements

In comparison, steady-state amplitude measurements can be easily performed, due to the greatly increased sensitivity of the equipment. LF and HF pump intensity measurements show that the LF/HF intensity ratio is constant ($\approx 10^{-3}$, Fig. 15), independent of pump intensity from threshold well into instability saturation, in disagreement with expectations from linear theory. Thus, the relative significance of LF and HF field intensities are virtually unaffected even by saturation effects; i.e., low frequency instability intensities always remain small in comparison to HF intensities. Having established the relation between HF and LF intensities, one need only determine the dependence of instability intensity upon pump intensity to evaluate completely the relationship between pump and instability (Fig. 16). Near threshold, the instability intensity increases strongly with pump intensity in agreement with the theory ($E_{inst}^2 \propto (1/\gamma)$) of parametric enhancement of HF and LF thermal fluctuations.¹⁰ Saturation (not present in linear theory) occurs when instability and pump intensities are comparable, with $\langle E_{inst}^2 \rangle \propto E_o^2$. Existing saturation theories¹¹⁻¹⁴ do not account for this dependence.

Power Balance

The significance of these results with respect to pump depletion and total power absorption is shown in Fig. 17(a). Below threshold, (or, equivalently, before instability growth), $P_{\text{abs}} \propto E_0^2$, as expected, since classical RF electron heating of the plasma is the dominant loss mechanism under these conditions. Increasing P_{abs} above threshold leads to instability onset and pump depletion (consistent with the measured relation between pump and instability intensity). Fig. 17(b) shows that $P_{\text{abs}} \propto (E_0^2 + E_{\text{instHF}}^2)$, i.e., that the dominant loss mechanism is still (classical) RF heating of electrons, but that now a significant portion of the heating is done by the instability. Relating this enhancement to conditions just below threshold we introduce the well-known concept of anomalous resistivity

$$v_e^* = v_e \left(1 + \frac{\langle E_{\text{instHF}}^2 \rangle}{E_0^2} \right) \quad (7)$$

and evaluation of v_e^* only requires knowledge of the relation between instability and pump intensity-previously determined in Fig. 16. Thus the direct consequence of instability saturation is to limit the maximum anomalous RF resistivity (Fig. 18). Note that for the experimental conditions $v_{\text{emax}}^*/v_e \approx 10$.

The significance of this result to ionospheric plasma modification experiments is: (1) the parametric ion acoustic decay instability in an isothermal plasma causes a large increase in

total power absorption due to the presentation of a more resistive load to the incident RF heating power (reducing reflected power), and (2) the resistive enhancement is limited, due to instability saturation. The second result is in contrast to earlier cavity work,² where pump intensities were not sufficient to cause instability saturation.

Ion and Electron Heating

Ion Heating (See Ref. 3)

The significant results of this work are measurements of intense ion heating comparable to the electron heating, proportional to the energy density of the parametric ion acoustic decay instability, and the conclusive relation of this stochastic ion heating to the fluctuating electric fields of the ion-acoustic component of the decay instability. Ion-temperature rise times τ_H are longer, but of the order of the instability growth times ($1/\omega_{pi} < 1/\gamma < \tau_H \ll 1/\omega_{ci}$) and many orders of magnitude shorter than electron-ion collisional relaxation times, indicating that ion heating by the ion-acoustic decay instability is the only mechanism which can account for the observations. Ion heating rates agree reasonably well with computer simulations and with a simple theory.

Electron Heating

Electron temperature rise is due to classical RF heating by pump and HF instability field intensities, since essentially all

of the applied power absorbed by the plasma goes into heating of electrons. However, under all experimental conditions, electron thermal conductivity is very high; in addition, the Q-machine endplates act as infinite electron heat sinks, effectively preventing any significant increase in plasma electron temperature, maintaining $T_e/T_i \approx 1$. In a plasma where electron heat loss can be neglected, RF heating causes a rapid rise in T_e/T_i , causing significant reduction in acoustic Landau damping.

V. CONCLUSIONS

Review

The ion acoustic parametric decay instability has been conclusively identified in a plasma with $T_i \geq T_e$, by wavelength and frequency measurements. Threshold density dependence, instability intensity dependence upon pump intensity near threshold, HF and LF spectra, instability growth rates and bandwidths ($\Delta\omega \approx \omega_{LF}/2 \approx v_{iLD}$) are all in good agreement with coherent, homogeneous theory.

Other measurements appear not to be in agreement with linear theory. First, the LF/HF intensity ratio is constant, over a wide range of pump intensities. Second, instability saturation occurs with $\langle E_{instHF}^2 \rangle \propto E_0^2$ when $\langle E_{instHF}^2 \rangle \approx E_0^2$.

Absorbed power measurements show that ($p_{tot.abs.}/\text{plasma vol.}$) = $p_{abs} \approx v_e [\langle E_{instHF}^2 \rangle + E_0^2]$; consistent with the picture of RF electron heating by the HF fields as the dominant energy loss. Ion heating, by comparison, can be neglected, since $\langle E_{instLF}^2 \rangle / \langle E_{instHF}^2 \rangle \ll 1$. Other measurements show that the anomalous RF resistivity, and thus the absorption, v^* ($v^* = v_e [1 + \langle E_{instHF}^2 \rangle / E_0^2]$), can be an order of magnitude above the classical value.

Significance to Ionospheric Program

What significant points can be derived from the results regarding the ionospheric heating? First, the isothermal parametric ion acoustic decay instability is very effective in enhancing absorption (as well as causing pump depletion) of incident RF waves, leading to more efficient heating than in the absence of the instability. Due to the broad bandwidth of the instability spectra, in contrast to the case where $T_i \ll T_e$, observations show that the instability does not excite new parametric acoustic decay instabilities (i.e., cascading), even for $E_0/E_{oc} \approx 20$. Hence the anomalous absorption is due only to the HF field of one instability. This means, that with instability saturation, anomalous resistivity (per unit volume) also saturates. The saturated value is quite large: $\approx 10 \nu_e$. Second, most of the absorbed energy is deposited in the electrons, even though acoustic waves are severely ion Landau damped. Third, if heating pulses are long enough for instability saturation, $\tau \approx f_{pi}^{-1}$, electron heating rates for a given pump intensity are increased $\approx 10 \times$ over classical levels, due to anomalous resistivity (more efficient power absorption). Likewise, ion heating rates are also increased substantially on the τ time scale by the factor ω_{LF}/ν_{icoll} (since $\Delta\omega_{LF} \approx \omega_{LF}$), due to stochastic ion heating by the random acoustic fields of the parametric ion acoustic decay instability. Fourth, observed density reduction

due to plasma heating may have little relevance to the ionosphere, where the plasma is weakly ionized.

ACKNOWLEDGMENT

This work was supported by Defense Advanced Research Projects Agency Contract F30602-73-0163.

REFERENCES

- ¹T. K. Chu, A. W. Hendel and J. M. Dawson, Comments on Modern Physics, Part E, Comments on Plasma Physics and Controlled Fusion, Vol. I, No. 4 (1972).
- ²T. K. Chu and H. W. Hendel, Phys. Rev. Lett. 29, 634 (1972).
- ³H. W. Hendel and J. T. Flick, Phys. Rev. Lett. 31, 199 (1973).
- ⁴F. W. Perkins and P. K. Kaw, J. Geophys. Res. 76, 282 (1971).
- ⁵I. Katsumata and M. Okazaki, Jap. J. Appl. Phys. 6, 123 (1969); R. Motley and T. Kawabe, Phys. Fluids 14, 1019 (1971).
- ⁶Much theoretical work has been reported in this area. Two publications are especially illuminating, since they relate the instability to a pair of weakly coupled HF, LF harmonic oscillators: K. Nishikawa, J. Phys. Soc. Jap. 24, 916 and 152 (1968).
- ⁷Linear mode conversion is described in detail in: V. L. Ginzberg, Propagation of Electromagnetic Waves in Plasma (Gordon and Breach, New York, 1961).
- ⁸B. D. Fried and R. W. Gould, Phys. Fluids 4, 139 (1961); R. W. Gould, Phys. Rev. 136, 991 (1964).
- ⁹When $\rho_{Li}/a \ll 1$ finite plasma effects can be neglected: A. Y. Wong, Phys. Fluids 9, 1261 (1966).
- ¹⁰Theoretical results for the isothermal ion acoustic decay instability are given in : F. W. Perkins, C. Oberman and

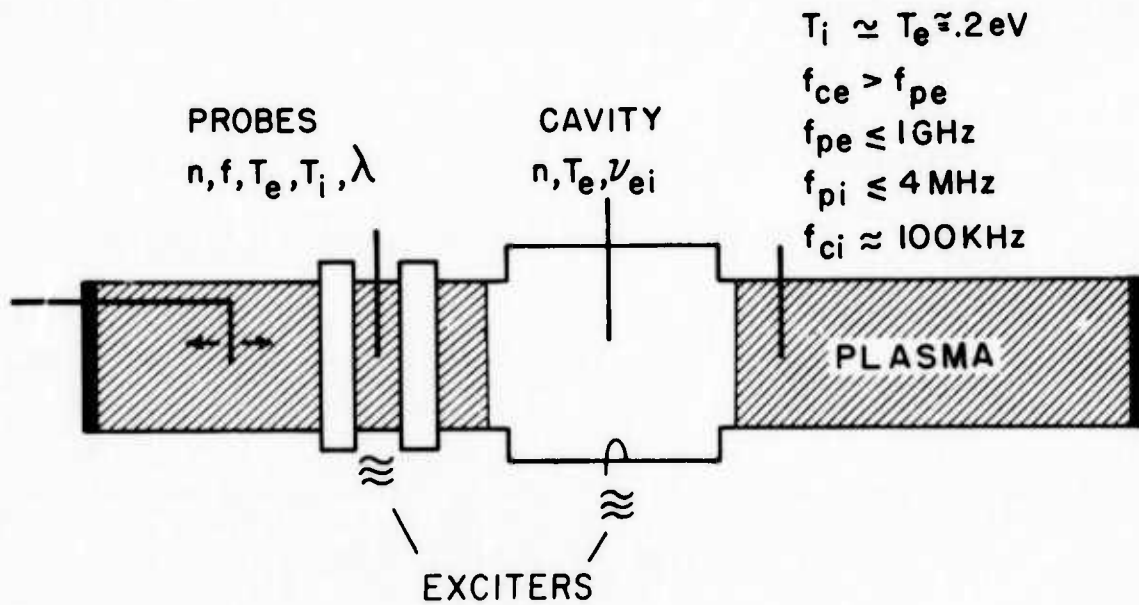
E. J. Valeo, Princeton Plasma Physics Laboratory Report PPL-AP69 (1973). A more physical derivation of the desired result can be found in: L. D. Landau, Acad. Sci. URSS 44, 311 (1944).

¹¹E. Valeo, F. Perkins and C. Oberman, Phys. Rev. Lett. 28, 340 (1972).

¹²D. F. Dubois and M. V. Goldman, Phys. Rev. Lett. 28, 218 (1972).

¹³J. S. DeGroot and J. I. Katz, Phys. Fluids 16, 401 (1973).

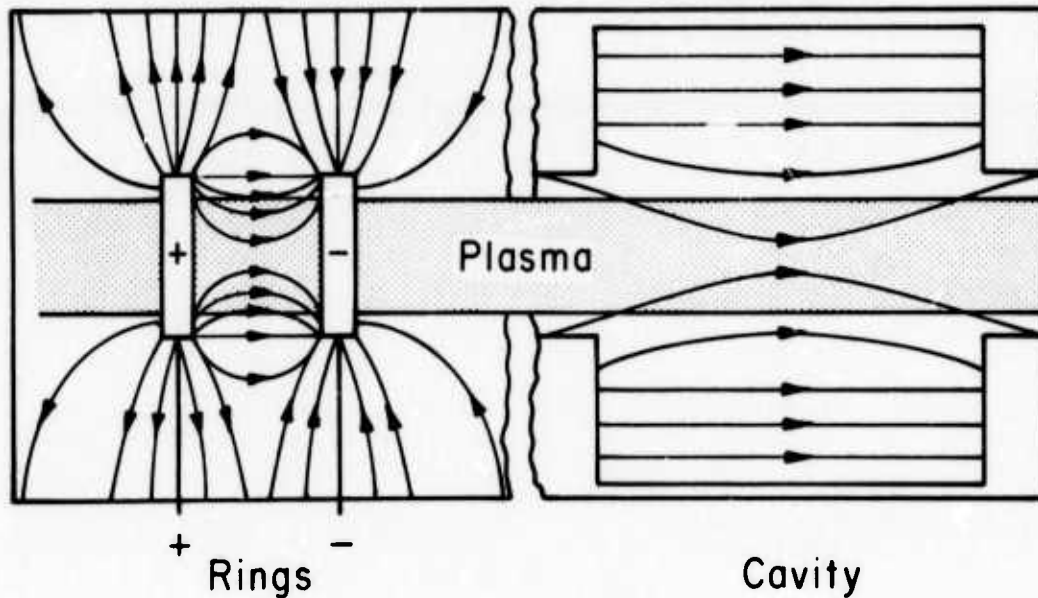
¹⁴B. Bezzerides and J. Weinstock, Phys. Rev. Lett. 28, 481 (1972).



743184

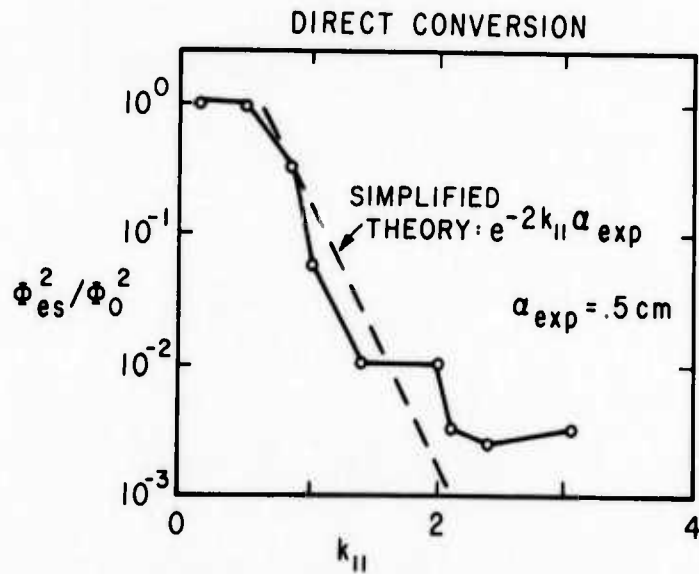
Fig. 1. General machine configuration, showing typical plasma parameters.

APPLIED PUMP FIELD STRUCTURE



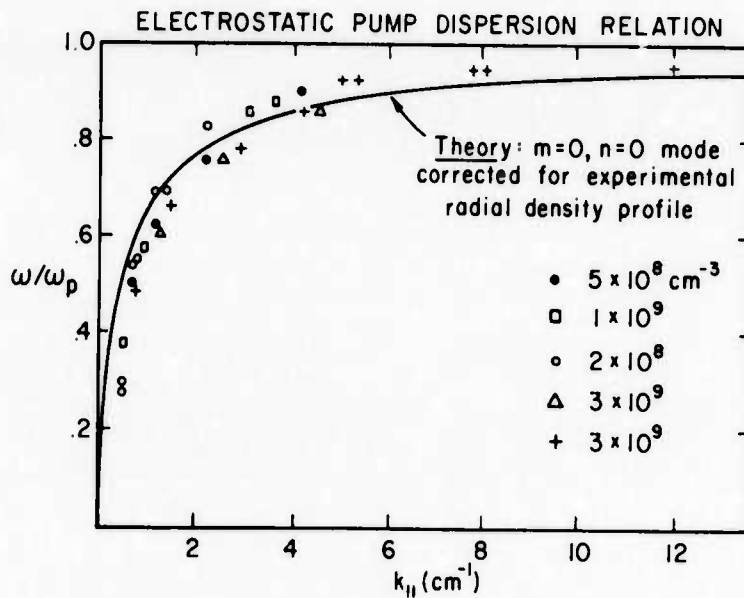
743185

Fig. 2. Pump field configuration: (a) Capacitive ring structure, (b) RF cavity. Perturbation effects due to plasma can be neglected, since the collisionless skin depth $c/\omega [1 - (\omega/\omega_{pe})^2] \gg a_{\text{plasma}}$.



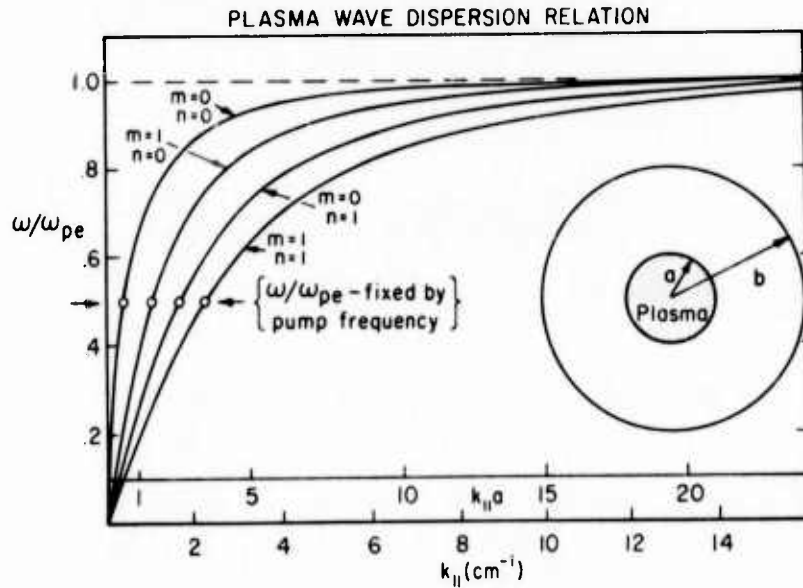
743188

Fig. 3. Direct (linear mode) conversion of pump field into $m = n = 0$ electrostatic Gould Trivelpiece plasma waves E^l , due to axial field gradients. Comparison is made to a simple theory: $\bar{n}_0(z) = [E_0/1 + (z/\alpha)^2]$
 $\rightarrow E^l(k_{||}\alpha) \cong e^{-k_{||}\alpha}$.



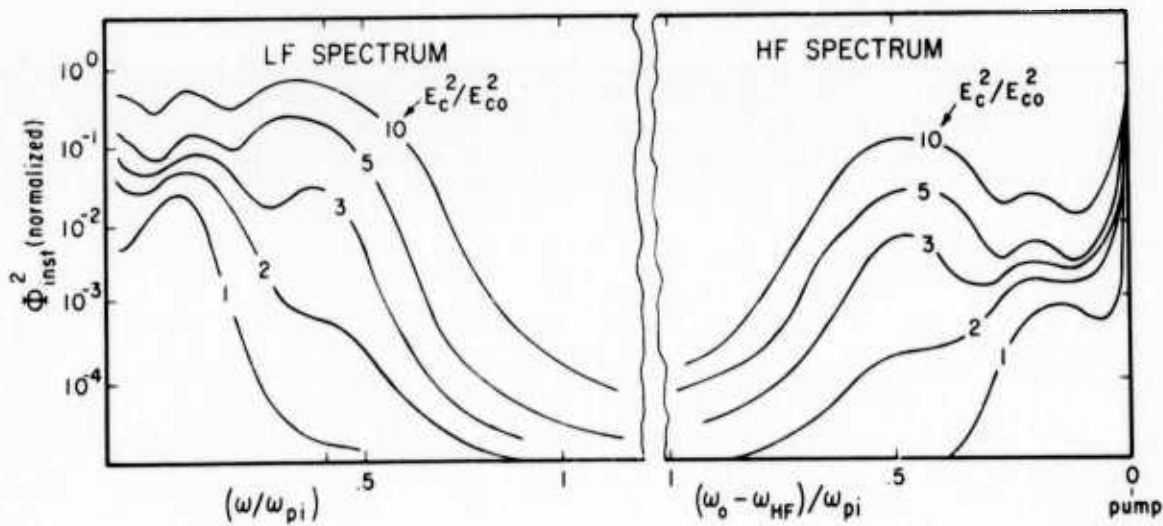
743189

Fig. 4. Dispersion relation of converted pump field, showing good agreement with theory for an $m = n = 0$ Gould-Trivelpiece (lower hybrid branch $-\omega_{pe}/\omega_{ec} < 1$) plasma wave, corrected for radial density profile.



743180

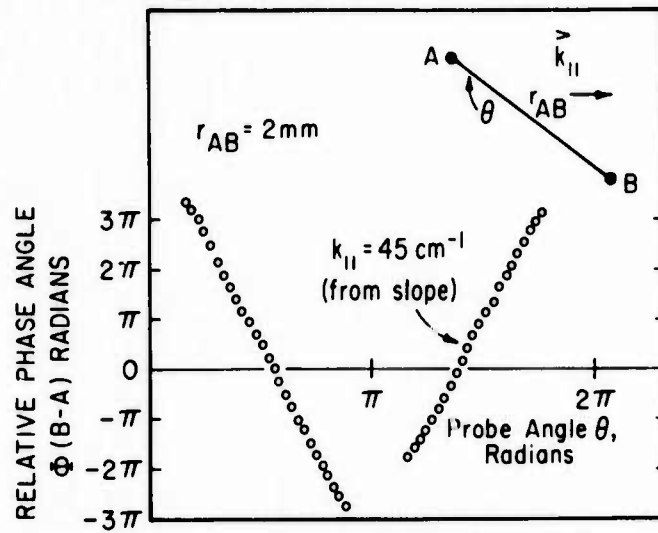
Fig. 5. General plasma wave dispersion relation, showing effects due to different mode numbers. In the limit $m, n \rightarrow \infty$ this reduces to the infinite plasma case, $\omega^2 = \omega_{pe}^2 (k_{||}/k)^2$ when $k_{||} \lambda_{de} < 1$. $n = 10^{10} \text{ cm}^{-3}$, $a = 1.5 \text{ cm}$, $b = 7.5 \text{ cm}$, $T_e = 0.2 \text{ eV}$.



743192

Fig. 6. Typical instability spectrum, showing detailed frequency matching, as expected from theory, $\omega/\omega_{pe} = 0.3$, $n = 10^{10}$, $B = 2 \text{ KG}$, $T_e \approx T_i/2 = 0.2 \text{ eV}$.

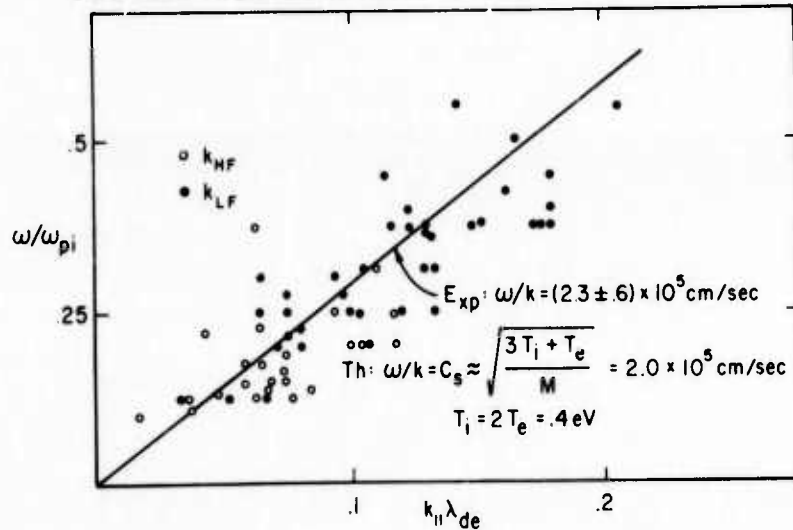
TYPICAL ACOUSTIC WAVELENGTH MEASUREMENT



743177

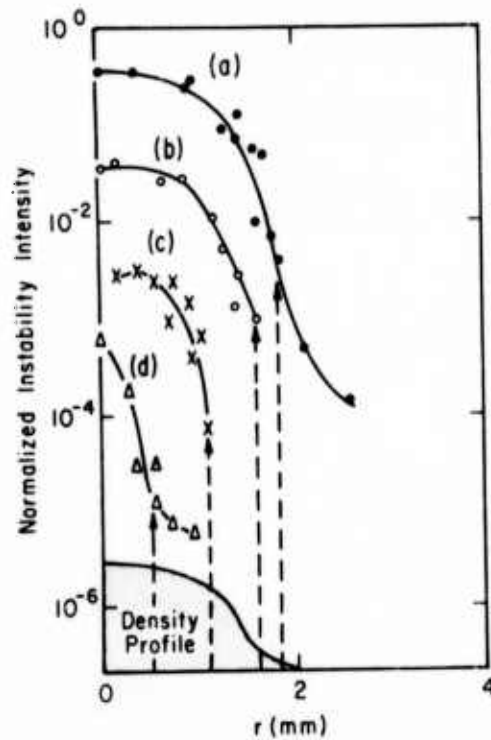
Fig. 7. Typical acoustic wavelength measurement, showing spatial coherence. $\omega_{LF}/\Delta\omega \approx 3$ ($\Delta f = \Delta\omega/2$ = instab. bandwidth), $\omega/\omega_{pe} = 0.95$, $n = 3 \times 10^9$, $B = 2$ KG, $T_e \approx T_i/2 = 0.2$ eV.

DISPERSION RELATION OF ACOUSTIC WAVES (momentum conservation)



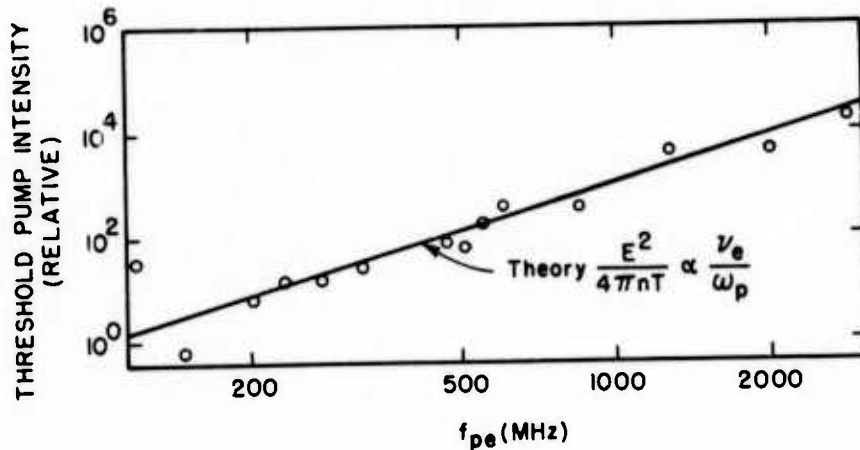
743182

Fig. 8. Normalized acoustic LF dispersion relation. Included are HF wavelength measurements, showing momentum conservation ($k_0 \approx 0$; $k_{HF} = -k_{LF}$) $\cdot \omega_{LF}/\Delta\omega \approx 3$, $n = 1 \times 10^{10}$, $B = 2$ KG, $T_e \approx T_i/2 = 0.2$ eV.



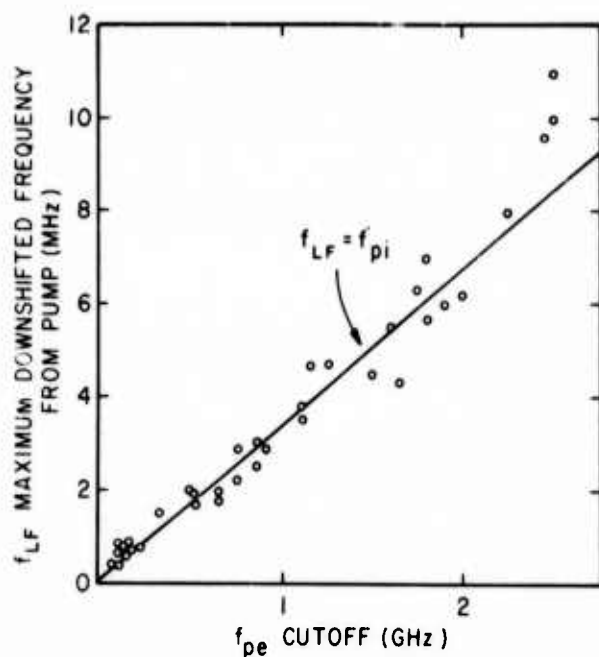
743183

Fig. 9. Instability radial profiles, showing cutoff dependence upon ω/ω_{pe} , in agreement with theory. Normalized LF, HF profiles are plotted together, since they are nearly equal. (a) $f_{LF} = 100$ kHz, $\omega/\omega_{pe} = 0.25$; (b) $f_{LF} = 1.1$ MHz, $\omega/\omega_{pe} = 0.46$; (c) $f_{LF} = 1.5$ MHz, $\omega/\omega_{pe} = 0.8$; (d) $f_{LF} \cong 2$ MHz, $\omega/\omega_{pe} = 0.92$. $n = 10^{10}$, $B = 2$ KG. Dotted lines indicate theoretical radial cutoff.



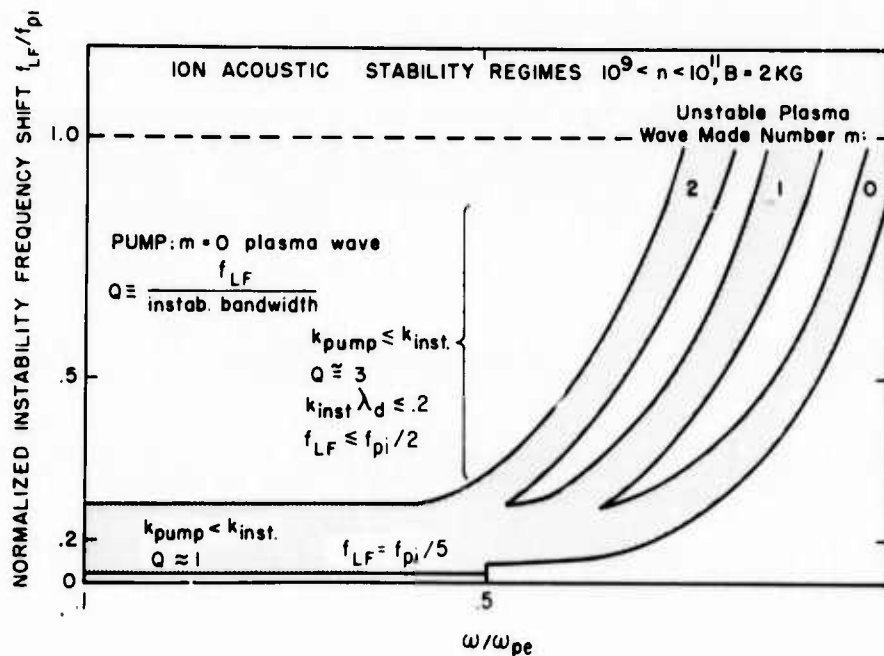
743187

Fig. 10. Density dependence of instability threshold, showing good agreement with theory. $k_0 \ll k_{inst}$, $\omega/\omega_{pe} = 0.4$, $B = 2$ KG.



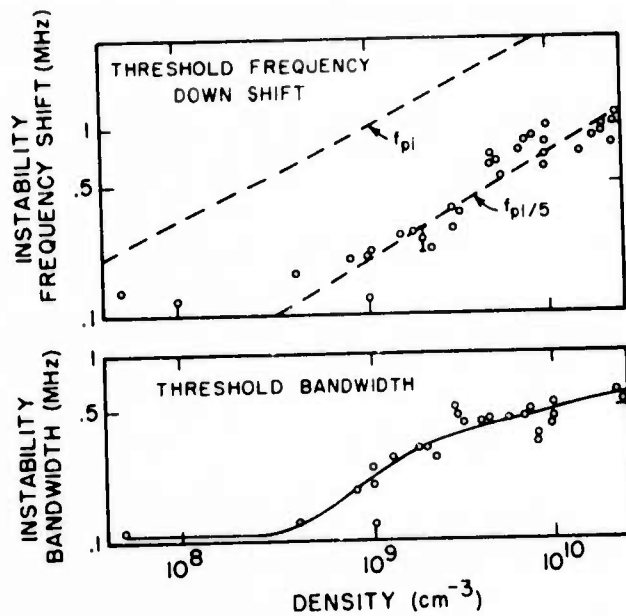
743186

Fig. 11. Maximum acoustic frequency (equivalent HF instability downshift from pump frequency) vs density, showing density dependence.



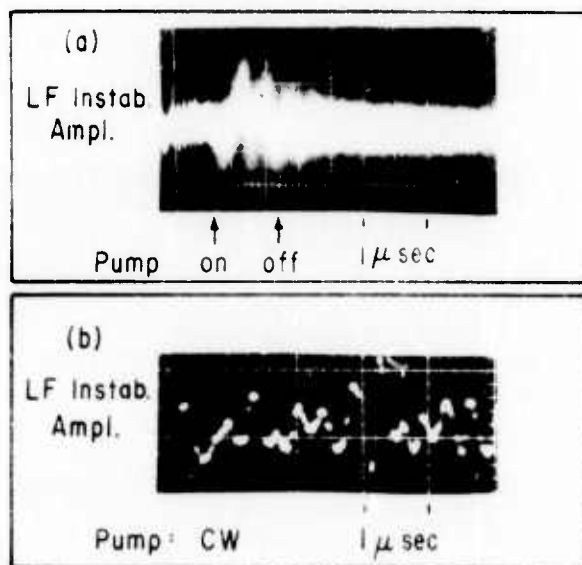
743178

Fig. 12. Overall view of ion acoustic decay instability regimes.



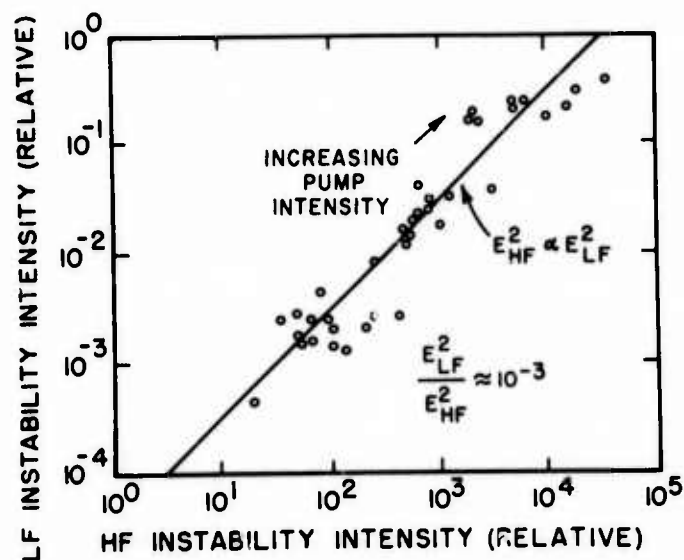
743176

Fig. 13. Density dependence of "electromagnetic" ($k_0 \ll k_{inst}$) ion acoustic decay instability. $v_e > \omega_{LF}$, $k_{inst} \lambda_d \approx 0.1$, $\omega/\omega_{pe} = 0.4$, $B = 2$ KG. $T_e \approx T_i/2 = 0.2$ eV.



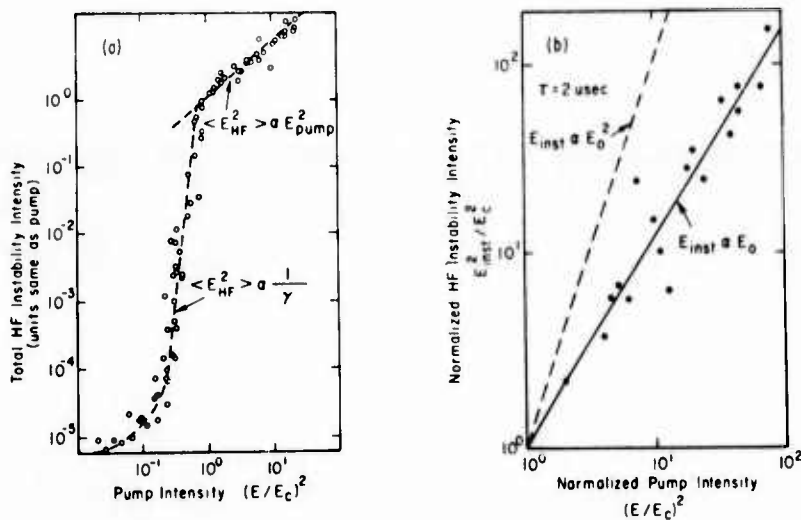
743193

Fig. 14(a). Temporal growth and decay of LF portion of instability, averaged over many pulses to show coherence. $f_{LF} \approx 3$ MHz, $\gamma \approx 3$ MHz; $v_{LF}/\omega_{LF} \approx 1/3$, $0.5 \mu\text{sec}/\text{div}$. (b) Steady-state behavior of LF portion of instability (single trace only) showing incoherence. $f_{LF} \approx 3$ MHz, $\Delta f \approx 1$ MHz, $1 \mu\text{sec}/\text{div}$, $n = 10^{10}$, $B = 2$ KG.



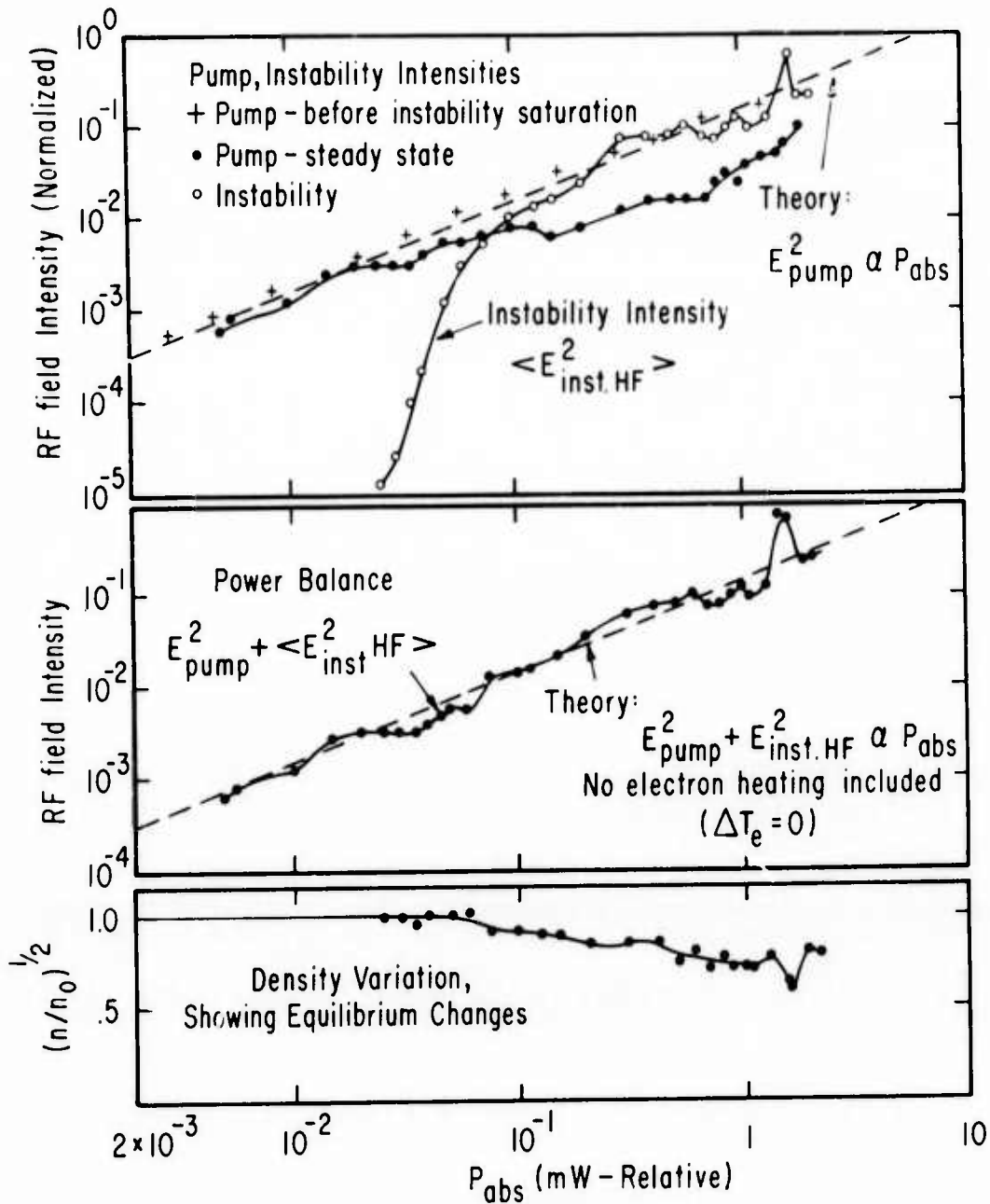
743190

Fig. 15. Relations between time-averaged, steady-state LF and HF instability intensities, showing direct proportionality. $f_{LF} \approx 700$ KHz, $\omega/\omega_{pe} = 0.3$, $n = 10^{10}$, $B = 2$ KG, $T_e \approx T_i/2 - 0.2$ eV.



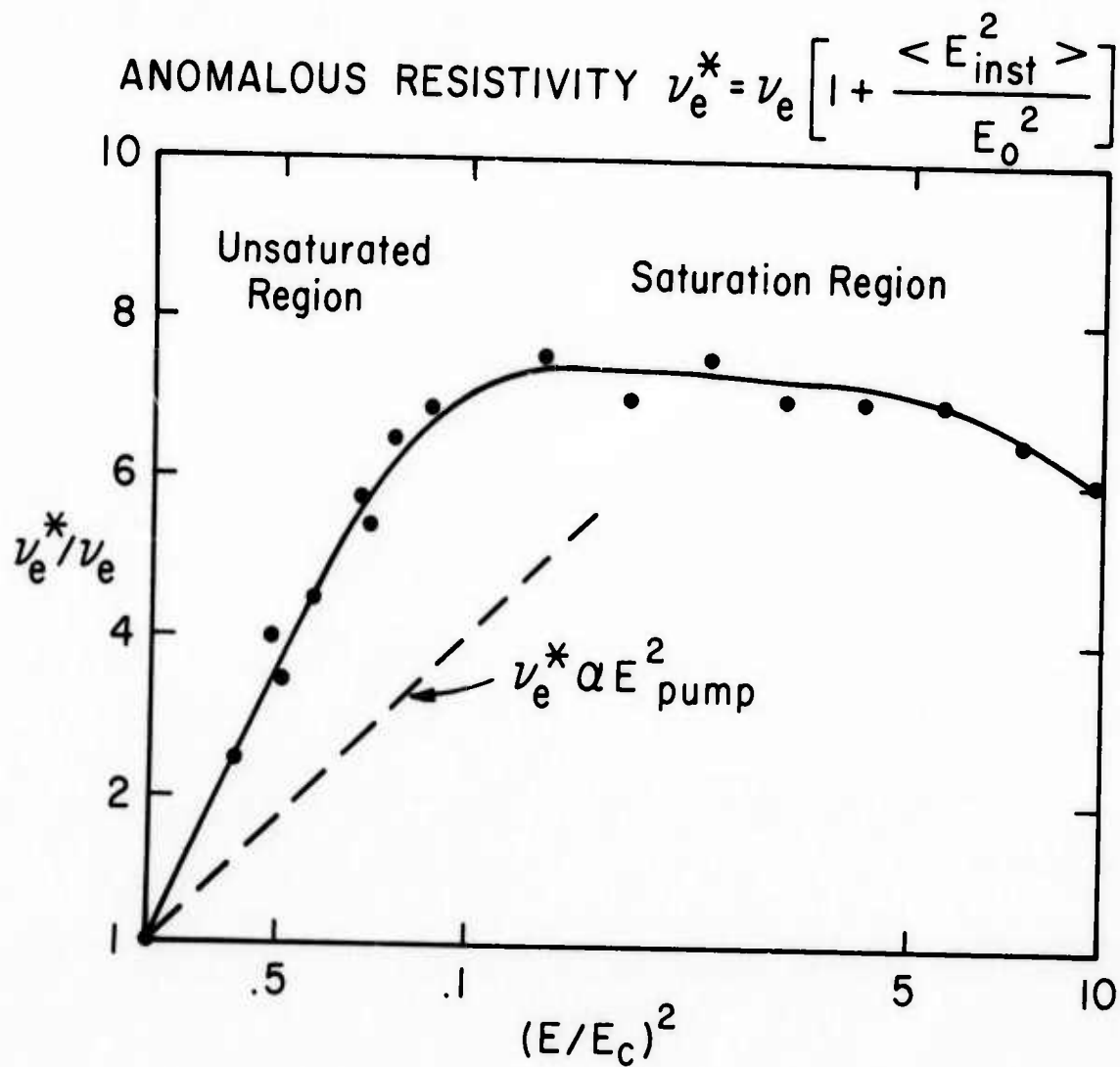
743191

Fig. 16. Dependence of instability intensity upon pump intensity. (a) Steady-state, showing growth out of critical fluctuations, and saturation. (Note definition of threshold as onset of saturation.) $f_{LF} = 2.6$ MHz, $\omega/\omega_{pe} = 0.8$, $n = 8 \times 10^9$, $B = 2$ KG, (b) Pulsed, just after instability saturation, but before equilibrium changes. $f_{LF} \approx 2$ MHz, $\omega/\omega_{pe} = 0.7$, $n = 10^{10}$, $B = 2$ KG.



743181

Fig. 17. Typical steady-state absorbed power measurements, showing relations between P_{abs} , pump and instability; P_{abs} and total HF field; P_{abs} and density. (Note pump depletion and anomalous absorption due to instability, indicated by shading.)
 $f_{\text{LF}} \approx 3 \text{ MHz}$, $\omega/\omega_{pe} = 0.8$, $n = 10^{10}$, $B = 2 \text{ KG}$,
 $T_e \approx T_i/2 = 0.2 \text{ eV}$.



743179

Fig. 18. Dependence of measured anomalous resistivity enhancement upon pump, showing saturation. Reduction in ν_e^*/ν_e at high pump levels is related to severe equilibrium changes.



MISSION
of
Rome Air Development Center

RADC is the principal AFSC organization charged with planning and executing the USAF exploratory and advanced development programs for electromagnetic intelligence techniques, reliability and compatibility techniques for electronic systems, electromagnetic transmission and reception, ground based surveillance, ground communications, information displays and information processing. This Center provides technical or management assistance in support of studies, analyses, development planning activities, acquisition, test, evaluation, modification, and operation of aerospace systems and related equipment.